$$F(0) = \frac{p_5 x_5^{11} + p_6 x_5^{12}}{p_5(x_2^{11} + x_3^{11} + x_4^{11}) + p_6(x_2^{12} + x_3^{12} + x_4^{12})}$$

$$F_e = \frac{1}{770} \cdot {}_{10}[-0.26 + 0.03\,(T(N) - 273)]$$

where:

$$\gamma = \frac{2\,p_5(x_2^{11} + x_3^{11} + x_4^{11}) + 2\,p_6(x_2^{12} + x_3^{12} + x_4^{12})}{p_5(x_2^{11} + x_3^{11}) + p_6(x_2^{12} + x_3^{12})}$$

and N is a spatial variable of the absorber vessel. The integrals occurring in (9B), (13B), and (14B) were evaluated numerically.

Cooler No. 3

$$x_1^6 = x_1^{13} = P_2 \tag{17B}$$

$$x_2^6 = p_7 \cdot x_2^8 \tag{18B}$$

$$x_3^6 = p_7 \cdot x_3^8 \tag{19B}$$

Cooler No. 4

$$x_1^{12} = x_1^{14} \tag{20B}$$

$$x_2^{12} = (1 - p_7)x_2^8 \tag{21B}$$

$$x_3^{12} = (1 - p_7)x_3^8 \tag{22B}$$

Cooler No. 6

$$x_1^2 = x_1^{15} = p_3 \tag{23B}$$

$$x_2^2 = 0.117\,x_2^1 \tag{24B}$$

$$x_3^2 = 0.117\,x_3^1 \tag{25B}$$

$$x_4^2 = 0.117\,x_4^1 \tag{26B}$$

$$x_5^2 = 0.117\,x_5^1 \tag{27B}$$

Cooler No. 7

$$x_1^{11} = x_1^{16} \tag{28B}$$

$$x_2^{11} = x_2^4 \tag{29B}$$

$$x_3^{11} = x_3^4 \tag{30B}$$

Pump No. 5

$$-x_1^8 + \left[\frac{Q_7}{Q + p_2 Q_{11} + Q_9 + Q_{10}}\right]x_1^7 + \left\{\frac{P_2 Q_{11}}{Q_7 + p_2 Q_{11} + Q_9 + Q_{10}}\right\}x_1^{11} + \left\{\frac{Q_{10}}{Q^7 + p_2 Q_{11} + Q_9 + Q_{10}}\right\}x_1^{10} = 0 \tag{31B}$$

$$\left\{\frac{Q_9}{Q^7 + p_2 Q_{11} + Q_9 + Q_{10}}\right\}x_1^5$$

$$-x_2^8 + x_2^7 + p_2 \cdot x_2^{11} + x_1^9 + x_2^{10} = 0 \tag{32B}$$

$$-x_3^8 + x_3^7 + p_2 \cdot x_3^{11} + x_3^{10} = 0 \tag{33B}$$

where:

$$Q_7 = 18\,x_2^7 + 17\,x_3^7$$

$$Q_{11} = p_2(18\,x_2^{11} + 17\,x_3^{11})$$

$$Q_9 = 18\,x_1^9$$

$$Q_{10} = 18\,x_2^{10} + 17\,x_3^{10}$$

Effects of Ultrasonic Vibrations on Heat Transfer to Liquids by Natural Convection and by Boiling

S. W. WONG and W. Y. CHON

McGill University, Montreal, Canada

The effects of ultrasonic vibrations on heat transfer to water and methanol by natural convection and by boiling were measured at three ultrasonic energy levels with frequency ranging from 20.6 to 306 kcycles/sec., using electrically heated platinum wires of diameters 0.007 and 0.010 in. Up to an eight-fold increase in heat transfer coefficient was obtained in natural convection, but the effects diminished with increased temperature difference and became negligible in the well-developed nucleate boiling region. High-speed photographs showed that the increase was due to the motion of cavitation bubbles on the wire surface. The heat transfer results were correlated by local cavitation activity values measured by a technique developed for this work.

Acoustic cavitation usually refers to the formation of small bubbles and their subsequent growth and collapse within a liquid sound field. Such cavitation bubbles can be used to create disturbances in the relatively stagnant film of liquid near a heating surface as well as to increase the bulk mixing in the liquid. Thus up to a four-fold increase in natural convective heat transfer coefficient was reported by Larson and London (*1*). Similar study by Robinson, et al. (*2*), however, showed that the increase was less than 20%. Direct comparison of published data is usually impossible because of the various methods used to measure and report the acoustic properties of the system. The effects of ultrasonic vibrations in many cases may also depend on the location of the heating surface in the ultrasonic field. The results will be strongly dependent on the geometry of the test system.

The limited number of papers published on the effects of ultrasonic vibrations on boiling heat transfer is mainly concerned with the increase of burnout heat flux. Isakoff (*3*) appears to be the only investigator to have studied the effect on nucleate pool boiling and reported that the range of nucleate boiling could be considerably extended. Romie and Aronson (*4*) as well as Ornatskii and Shcherbakov (*5*) suggested that the effect of ultrasonic vibrations would be to reduce the mean bubble size and to increase the frequency of bubble formation. No experi-

---

S. W. Wong is with Imperial Oil Limited, Calgary, Alberta, Canada. W. Y. Chon is at the State University of New York at Buffalo, Buffalo, N. Y.

mental work has been done to confirm these points.

The purpose of this study is to establish the important variables and mechanisms of these heat transfer processes, and to correlate the heat transfer results with local cavitation activity values measured by a technique recently developed (*6*).

EXPERIMENTAL APPARATUS AND PROCEDURE

A schematic diagram of apparatus is shown in Figure 1. Two types of transducers were used in this study, namely, magnetostrictive transducers for frequencies of 20 and 44 kcycles/sec. and ceramic transducers for frequencies of 108 and 306 kcycles/sec. The transducers which were cemented directly onto the bottom of an open stainless steel tank (7½ × 4½ × 6 in. deep) were driven by a sine-wave form signal generator whose output was amplified by a custom-built power amplifier. The amplifier had a frequency range of 15 to 500 kcycles/sec. with a power output rating of 200 w. A standard resistor was connected in series with the transducers to measure the current of the circuit. The apparent electrical power (W_A) to the transducers was then calculated to be the product of the effective values of the current and the voltage drop across the transducers. No attempt was made to determine the power factor of the circuit.

Electrically-heated platinum wires of 0.007 in. and 0.010 in. diameter were used as the heating element as well as resistance thermometer. In order to minimize end conduction effects, only the central portion (approximately ¾ in. long) of the heating element was made to serve as the test section by the use of platinum potential leads having smaller diameters (0.002 in. and 0.0045 in.). The heat transfer rates were calculated from the voltage drop across and the current through the test section. The voltage drops across the standard resistor and the test section were measured with a potentiometer-galvanometer combination capable of reading to 0.01 mv. at 1 mv.

Distilled water and methanol were used in this study. The temperature of the liquid was maintained to within 1°F. by three strip heaters on the sides of the tank. A glass window was installed on the front of the tank so that a high-speed photographic study of the heat transfer processes could be made.

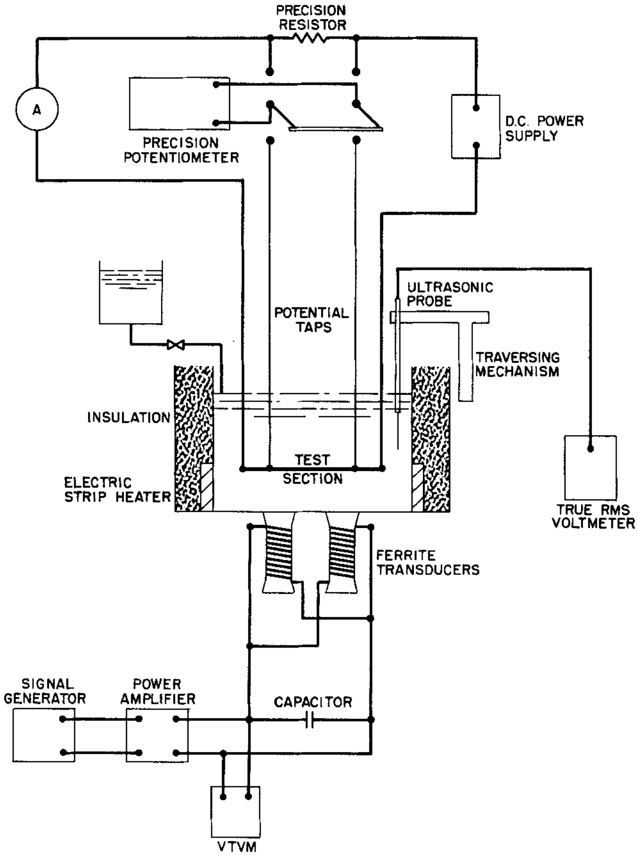

Fig. 1. Schematic diagram of apparatus.

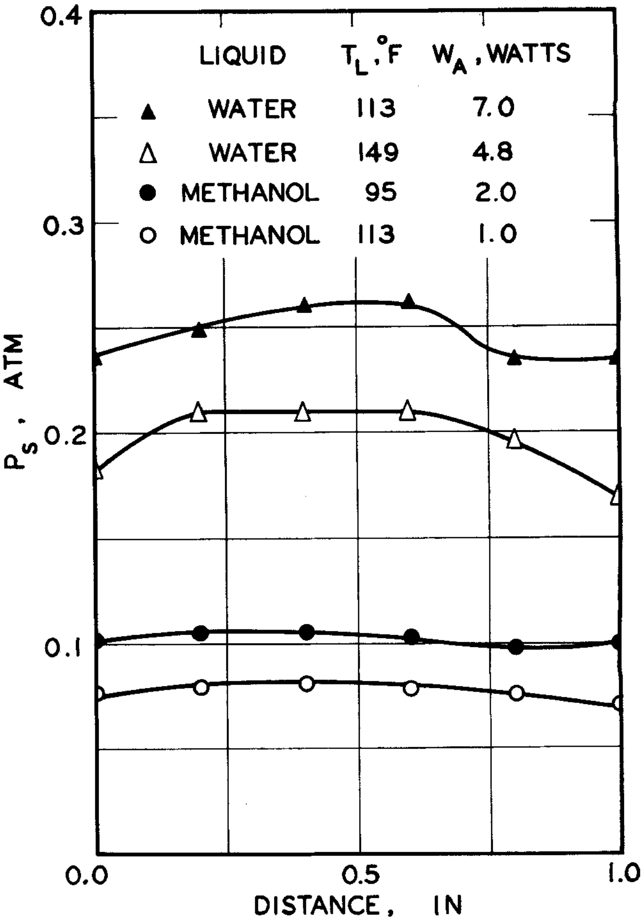

Fig. 2. Some typical sound pressure profiles on the cavitation damage specimen.

In all experiments the liquid temperature was always brought up slowly so that the dissolved air content in the test liquid would be at its equilibrium value. No measurement was made of the air content of the liquid.

To measure the liquid ultrasonic field, a specially prepared specimen, which is an 18 gauge copper wire, 1½ in. long, coated with a soil containing cobalt 60, was first mounted in the same location as the wire in Figure 1. When the applied ultrasonic energy was below the cavitation threshold of the liquid, the root-mean-square values of sound pressure along the specimen were measured at equal intervals of 0.02 in. by a Gulton Glennite ultrasonic probe whose sensitive element is a 1/16 × 1/16 in. barium titanate cylinder. The calibration of the probe was supplied by the manufacturer. Some typical sound pressure profiles on the specimen are shown in Figure 2. The reproducibility of the sound pressure measurements was always within 5%. For energy levels above the cavitation threshold, the cavitation activity of the ultrasonic field was measured in terms of the percentage of soil removed. The percentage of soil removed is the ratio of the counting rate of a damaged specimen by cavitation to that of the same specimen unexposed to the ultrasonic field (*6*). The heat transfer data with and without ultrasonic vibrations in natural convection and nucleate boiling region were taken after the ultrasonic fields at various apparent electrical power inputs to the transducers were measured. When the frequency was 20.6 kcycles/sec., two liquid temperatures were used for each liquid, namely 113°F. and 149°F. for distilled water and 95°F. and 113°F. for methanol. For higher frequencies, the temperature of distilled water was 149°F. and that of methanol was 113°F. These temperatures were selected so that no vapor bubbles were formed on the tank walls. Preliminary experiments showed that the motion of these vapor bubbles interfered with the ultrasonic field and rendered the measurements of sound pressure on the wire very difficult.

During the measurement of heat transfer data with ultrasonic vibrations, it was observed that the potential across the test section of the heating element was constant until at some apparent electrical power value, a sudden drop was recorded indicating a decrease in the wire temperature. Simultaneously, cavitation bubbles appeared on the wire. These cavitation bubbles were very unstable and began to roll on the wire surface soon after they were formed. The average value of sound pressure on the wire measured at that value of apparent electrical power is called the critical sound pressure. It was calculated by taking the square root of the average of the squares of individual root-mean-square sound pressure on the wire.

The critical sound-pressure can be defined as the sound pressure at which the applied ultrasonic field begins to have an effect on heat transfer. For sound pressures below the critical value, the rate of heat transfer was the same as in the case where there was no vibration. It was observed that the critical sound pressure was a function of liquid temperature, wire temperature, as well as the frequency of the ultrasonic field. In order that the heat transfer results could be compared directly, it was necessary to select values of apparent electrical power so that over the range of wire temperature used, the resulting sound pressures on the wire would exceed their corresponding critical values. A standard procedure was developed for determining the critical sound pressure and was given elsewhere (7). Some typical temperature history curves during the determination of critical sound pressures are given in Figure 3.

CRITICAL SOUND PRESSURE

The variation of critical sound pressure with wire temperature at the frequency of 20.6 kcycles/sec. for methanol at 95°F. and 113°F. is given in Figure 4.* The critical sound pressure shows a minimum in the temperature range of 170 to 180°F. corresponding to that for the incipience of boiling of methanol on the wire. Similar results were observed for distilled water.

It should be noted that at wire temperature below that for incipient boiling, the critical sound pressure is also the cavitation threshold of the liquid on the wire. Although the cavitation threshold of a liquid depends on both the gas content and vapor pressure of the liquid, the decrease in critical sound pressure over this wire temperature range indicates that vapor pressure is the controlling variable. This is because an increase in wire temperature would reduce the gas content of the liquid, and subsequently, would result in an increase rather than a decrease in critical sound pressure. The lower critical sound pressure values at higher liquid temperature also suggests that vapor pressure is more important. Consequently, at the incipience of boiling, little ultrasonic energy was necessary to induce the formation of cavitation bubbles. At wire temperatures above the incipient boiling, because of the vapor bubble activity from boiling, more ultrasonic energy was required to cause an increase in heat transfer. Since the vapor bubble activity was very sensitive to the wire temperature, a rapid increase in critical sound pressure resulted. In the well-developed nucleate boiling region where the effect of ultrasonic vibrations was negligible, the plots became asymptotic to critical sound pressure.

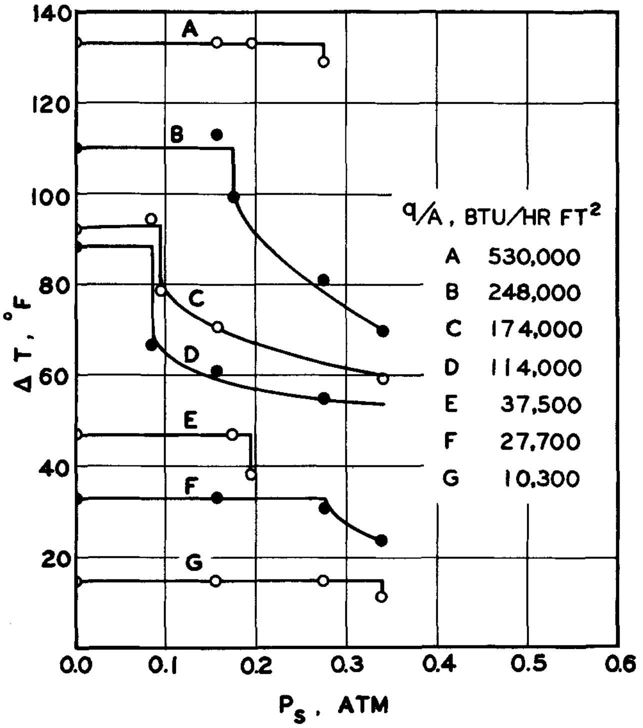

Fig. 3. Some typical temperature history curves during the determination of critical sound pressure.

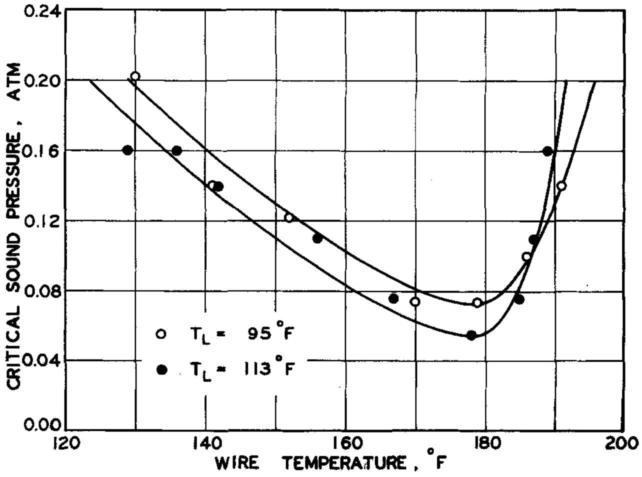

Fig. 4. Variation of critical sound pressure with wire temperature at 20.6 kcycles/sec. for methanol at 95°F. and 113°F.

The critical sound pressure values for methanol were observed to be about half of that for water. This can be attributed to its gas solubility which is more than an order of magnitude greater than the solubility of gas in water. The effect of frequency on critical sound pressure is shown in Figure 5. The increase is in accordance with the work of Esche (8) and Barger (9). Quantitative

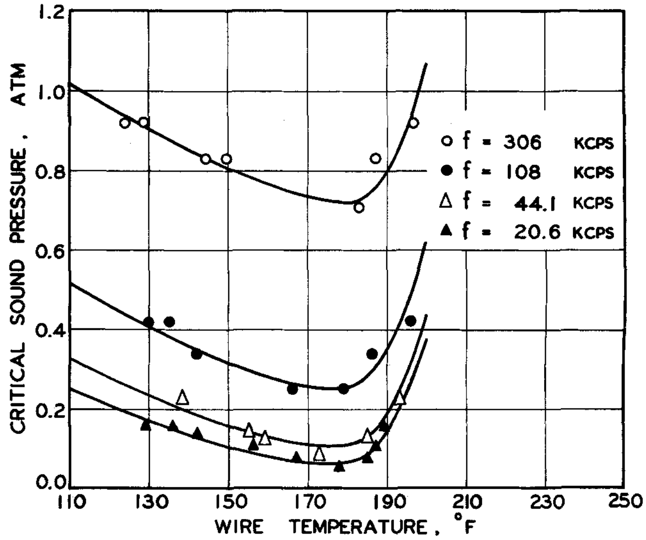

Fig. 5. Variation of critical sound pressure with wire temperature at different frequencies for methanol at 113°F.

---

* A total of 14 figures giving the critical sound pressure values for distilled water and those heat transfer data and correlations which are not included in this paper have been deposited as document NAPS-00289 with the ASIS National Auxiliary Publications Service, c/o CCM Information Sciences, Inc., 22 W. 34th St., New York 10001 and may be obtained for $1.00 for microfiche or $3.00 for photocopies. These figures are also available in the literature (7).

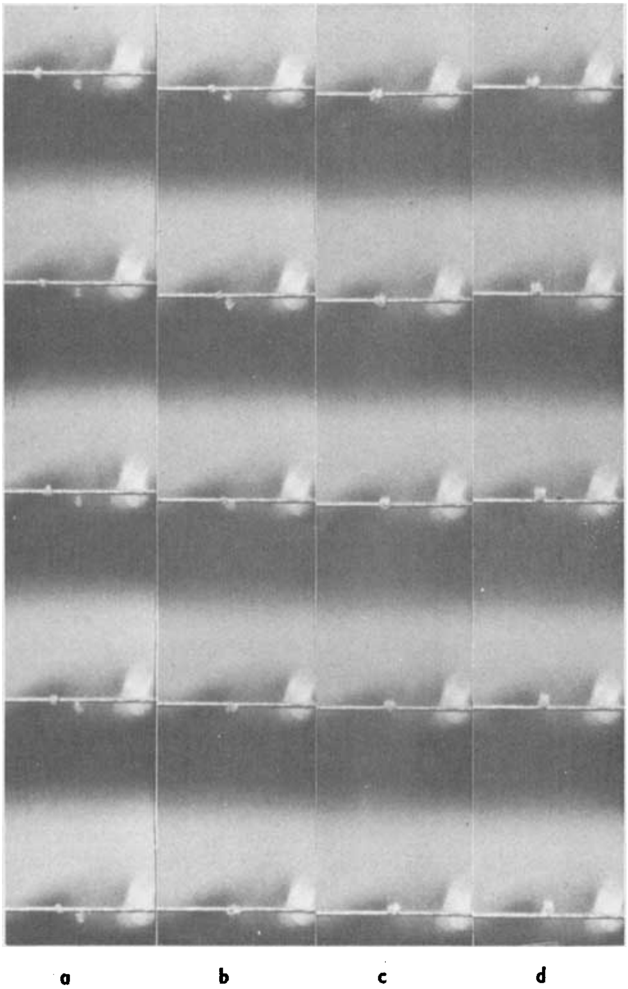

Fig. 6. Cavitation bubble motion on a heated wire.

comparison of their results with those obtained in this work cannot be made because the temperature and the state of liquid were different.

HIGH SPEED PHOTOGRAPHIC STUDY

A fastex high-speed 16 mm. camera was used in this study. High speed motion pictures at a framing speed of 4,000 frames/sec. were taken at four different conditions which are summarized in Table 1. Some representative frames were printed so that a detailed study of the bubble movements can be made. It should be noted that with $W_A = 36.2$ w., the resulting sound pressure exceeded the critical sound pressure as well as the cavitation threshold of the liquid. Subsequently, cavitation bubbles were formed both on the wire and in the bulk liquid. A summary of results is given in the following paragraphs. The detailed description of the cavitation bubble behaviors was given in (7).

1. It appeared that there was no preferential sites in the wire from which cavitation bubbles would grow. Small cavitation bubbles originated anywhere in the wire surface, rolled along the wire and grew in size by agglomerating with other smaller cavitation bubbles on the wire or that originated from the bulk liquid. The latter process is illustrated in Figure 6 taken for case A in Table 1. The lower bubble in the first frame of Figure 6*a* was a cavitation bubble originated in the bulk liquid and was migrating slowly toward the wire. The motion of cavitation bubbles on the wire surface was erratic and rapid. It was the result of the interaction of the bubbles with the ultrasonic field and further complicated by local temperature fluctuations of the liquid around the heated wire. Attempts to establish a pattern of the motion of cavitation bubbles on the wire were unsuccessful. Consequently it was impossible to determine the frequency of generation of cavitation bubbles. Figure 6 also shows that a cavitation bubble did not necessarily roll on the upper surface of the wire.

2. A high degree of radial oscillation in all cavitation bubbles as they rolled on the wire was observed. This is shown by the frosted appearance and the nonspherical shape of the cavitation bubble in Figure 6. In fact, it can be seen that the big cavitation bubble was composed of clusters of small bubbles sticking together. The clusters of bubbles would coalesce and become smooth and spherical only after they left the wire surface. The coalescence of bubbles is not illustrated in Figure 6. The increase in

TABLE 1. EXPERIMENTAL CONDITIONS SELECTED FOR HIGH SPEED PHOTOGRAPHY STUDY

Apparent electrical power input = 36.2 w.
Frequency of vibration = 20.6 kcycles/sec.
Filming speed = 4000 frames/sec.
Platinum wire diameter = 0.007 in.

	Test liquid	Liquid temperature °F.	Heat transfer coefficient B.t.u./hr. sq. ft. °F. without vibration	with vibration	Heat transfer region
A	methanol	113	451	850	natural convection
B	methanol	113	585	989	nucleate boiling (isolated bubbles)
C	methanol	113	2,060	2,060	nucleate boiling (well developed)
D	distilled water	149	1,890	4,180	nucleate boiling (isolated bubbles)

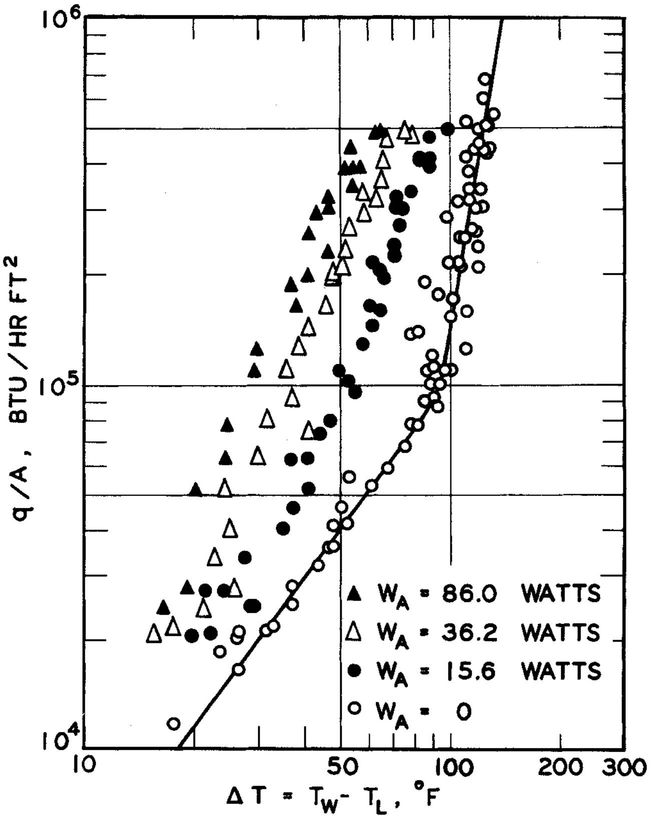

Fig. 7. Effect of 20.6 kcycles/sec. ultrasonic vibrations on heat transfer rates in distilled water at 149°F.

heat transfer can be explained as the result of the intense turbulence in the super-heated liquid layer on the heated wire, generated by the radial oscillations as well as the rapid and erratic motion of cavitation bubbles.

3. The activity of the cavitation bubbles increased with increasing wire temperature. It also depended on the gas solubility of the liquid which controlled the cavitation bubble content. The bubbles generated in water were observed to have collapsed on the wire surface. The high vapor content of these bubbles was the result of the relatively low value of gas solubility of water. The turbulence so generated was much more intense than that by the motion of the noncondensable cavitation bubbles generated in methanol whose gas solubility is an order of magnitude higher than that of water. This explains the higher increase in heat transfer obtained when water was used. As the wire temperature increased, the population of cavitation bubble also increased and their content changed from mainly gas to mainly vapor. The mechanism of heat transfer became similar to that of nucleate boiling without vibration.

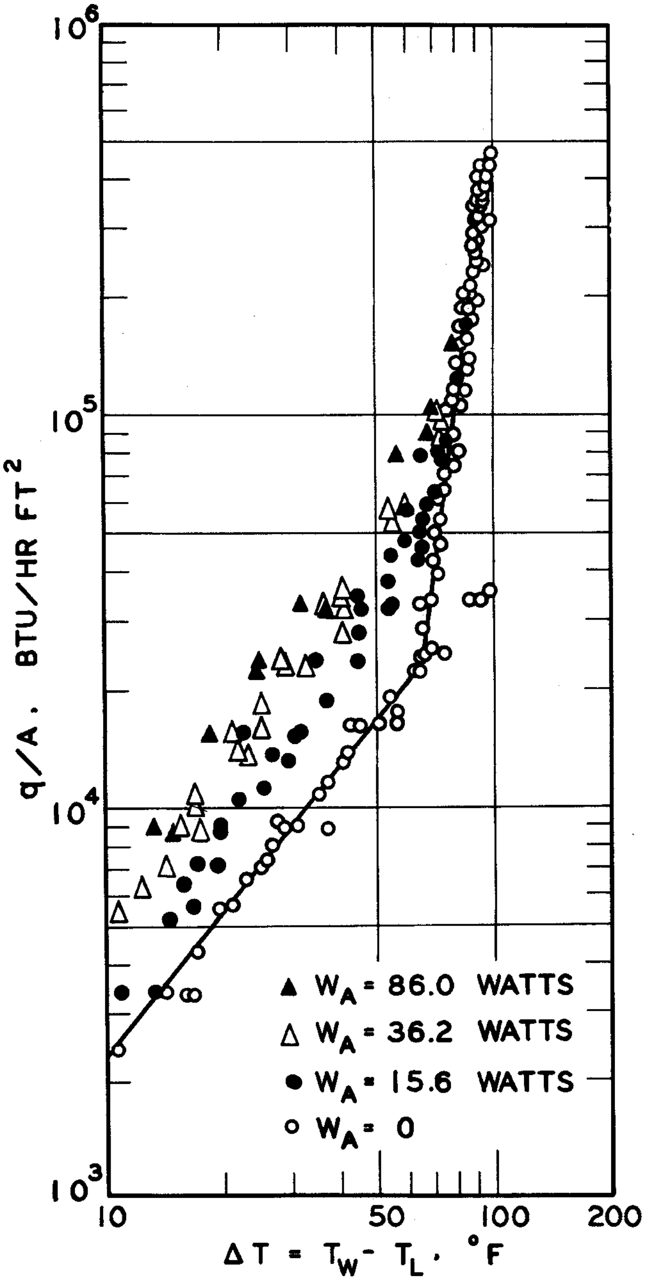

Fig. 8. Effect of 20.6 kcycles/sec. ultrasonic vibrations on heat transfer rates in methanol at 113°F.

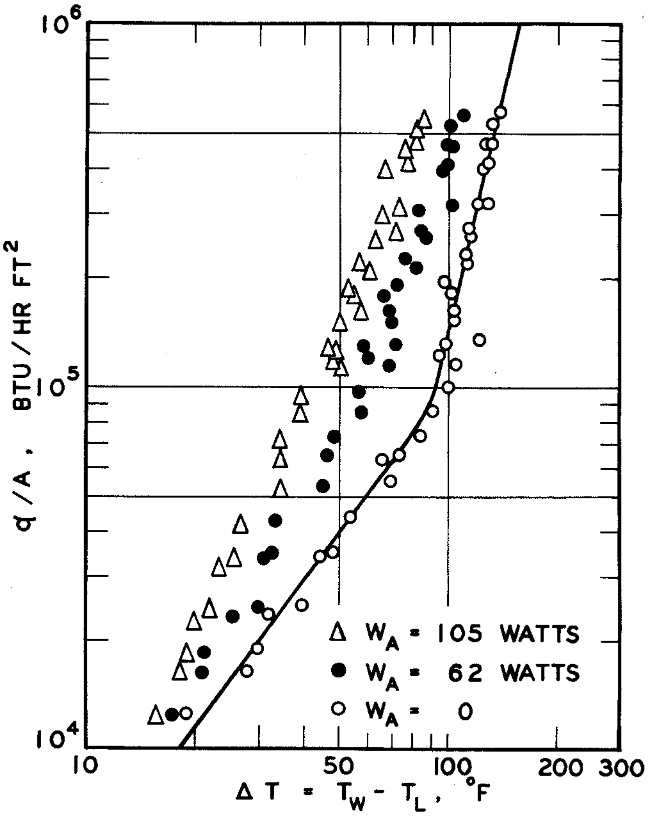

Fig. 9. Effect of 108 kcycles/sec. ultrasonic vibrations on heat transfer rates in distilled water at 149°F.

4. It was observed that the size of a cavitation bubble at which the erratic behavior of the bubble was first observed could be approximated by an equation which has been used to obtain the resonance size of an air bubble in a liquid sound field (*10*). It is given as follows:

$$R = \frac{1}{2\pi f}\sqrt{\frac{3\gamma P_o}{\rho_L}} \qquad (1)$$

HEAT TRANSFER RESULTS

Heat transfer results with ultrasonic vibrations at four different frequencies and each at three ultrasonic energy levels were obtained for distilled water and methanol. The effect of liquid temperature was also studied at 20.6 kcycles/sec. Some of the representative data are shown in Figures 7 to 10. Due to the instability of the boiling and cavitation phenomena, the errors could be as high as 5% in the values of heat flux and 2°F. in ΔT. The ΔT in all figures is the temperature difference between the platinum wire and the bulk liquid. The ultrasonic energy levels were expressed in terms of apparent electrical

TABLE 2. VALUES OF PERCENTAGE SOIL REMOVED AT WHICH HEAT TRANSFER DATA WERE MEASURED

Figure	Liquid	T_L °F.	f = 20.6 kcycles/sec. Percentage soil removed		
			W_A = 15.6 w.	W_A = 36.2 w.	W_A = 86.0 w.
7	distilled water	149	3.0	12.5	32.0
8	methanol	113	2.3	5.4	13.4
			f = 108 kcycles/sec.		
		T_L °F.	Percentage soil removed		
			W_A = 62 w.		W_A = 105 w.
9	distilled water	149	3.9		13.6
			f = 306 kcycles/sec.		
		T_L °F.	Percentage soil removed		
			W_A = 125 w.		W_A = 160 w.
10	methanol	113	2.9		7.6

powers to the transducers. The corresponding values of percentage of soil removed were given in Table 2.

Heat transfer experiments without vibration were performed in order to check the experimental techniques and to establish a reference relation with which to compare results when ultrasonic vibrations were used. For data in the natural convection region, the Grashof-Prandtl product and the Nusselt number were calculated and are presented as a plot of N_{Nu} vs. $(N_{Gr} \times N_{Pr})$ in Figure 11. The solid line is the best-fitted straight line for the data points and the dashed line is the recommended correlation for single horizontal cylinder in the same range of Grashof-Prandtl product (10 to 150) given by McAdams (*11*). The difference in Nusselt numbers from the two lines does not exceed 4%.

The effects of ultrasonic vibrations, as shown in Figure 7 to 10, were to increase the heat transfer rates, and hence the heat transfer coefficients at a given ΔT. Depending on the ultrasonic energy as well as the temperature difference, up to an 800% increase in heat transfer rates could be obtained. When the test liquid was methanol, regardless of the frequency of the ultrasonic field or the liquid temperature, the effects of ultrasonic vibrations diminished as the wire temperature was increased. At sufficiently high wire temperatures, the turbulence generated by the motion of cavitation bubbles could not exceed that from the growth and detachment (collapse) of vapor bubbles as in the well-developed nucleate boiling without vibration, no increase in heat transfer rate was observed. It is expected similar results would be obtained for distilled water if a D.C. power supply with a larger amperage output was used.

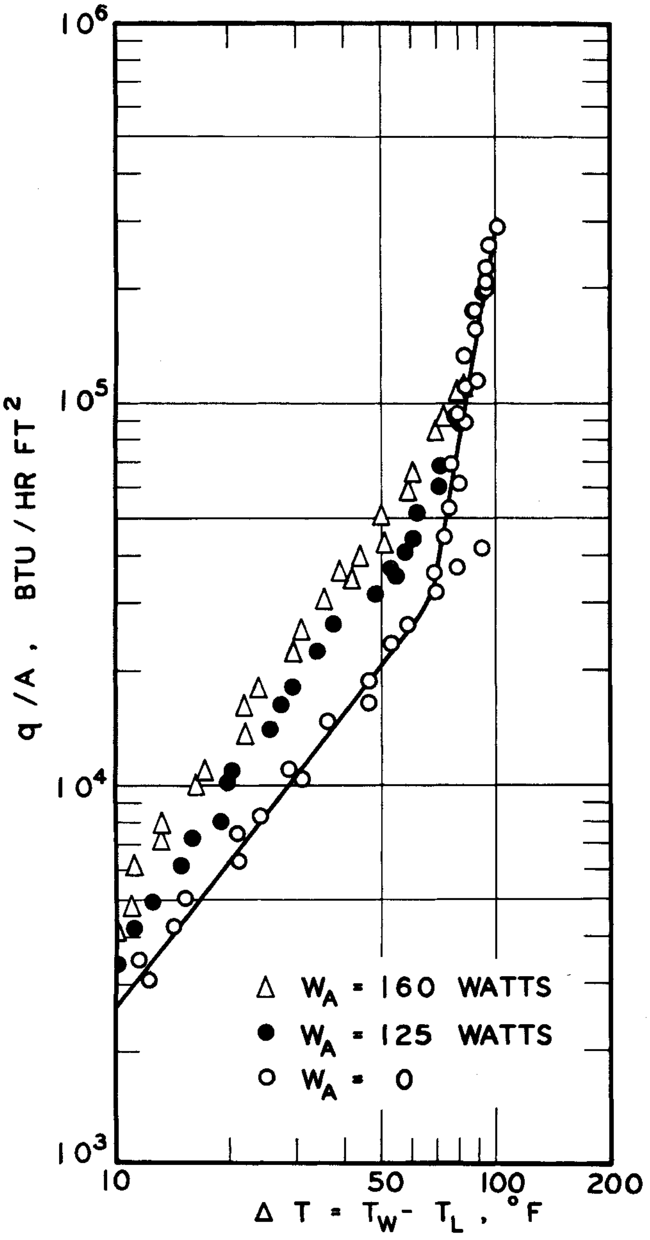

Fig. 10. Effect of 306 kcycles/sec. ultrasonic vibrations on heat transfer rates in methanol at 113°F.

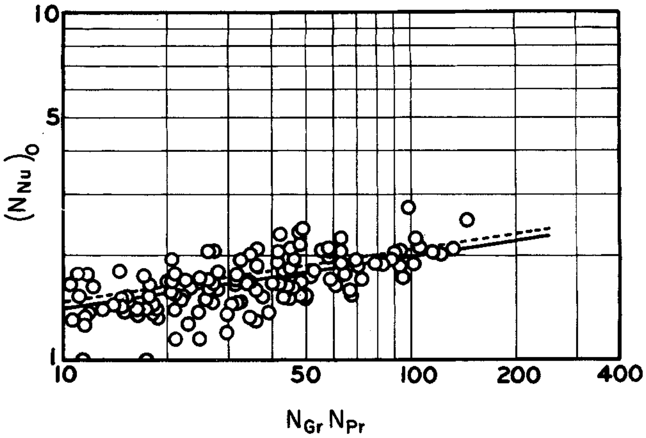

Fig. 11. Natural convective heat transfer from horizontal platinum wires to liquids.

A change in water temperature from 113 to 149°F. resulted in a change in the increase in heat transfer rates from 45 to 100% for approximately the same value of soil removal. Both heat transfer rates were evaluated at a temperature difference of 40°F. The critical sound pressure for water at 149°F. was much lower than that at 113°F. At the same value of soil removal, the liquid with a lower critical sound pressure showed increased cavitation bubble activity on the wire surface. Similar results were obtained for methanol.

The effect of frequency evaluated on the basis of percentage of soil removed was relatively unimportant. The increase in heat transfer rates at the same liquid temperature, the same temperature difference, and approximately the same value of percentage of soil removed was lowered from 100 to 70% for a five-fold increase in frequency. According to Equation (1), the resonance size of cavitation bubble was decreased by a factor of five as the frequency increased from 20.6 to 108 kcycles/sec. In order to have the observed effect on heat transfer, the small cavitation bubbles must be as efficient as the larger cavitation bubbles in creating turbulence in the liquid at the wire surface.

CORRELATION OF DATA

Attempts to correlate all heat transfer results with a single equation were unsuccessful. It was found, however, that the results at a single frequency and wire temperatures below the temperature for incipient boiling could be correlated by the following:

$$(N_{Nu})_w = C_1 \frac{{N_{Gr}}^{1/2} \, {N_{Pr}}^{1/2} \, {S_R}^{1/2}}{P_{CR}} + C_2 \qquad (2)$$

The data points taken at wire temperatures above that for incipient boiling were above the correlation. For each frequency, there was a set of C_1 and C_2 which were obtained by the least squares method. Two of the correlations are shown in Figures 12 and 13.

The results from high speed photographic study showed that the cavitation bubble activity and its content depended on the wire temperature. The soil removal measurements representing the cavitation activity at the heating surface, however, were conducted in liquids under

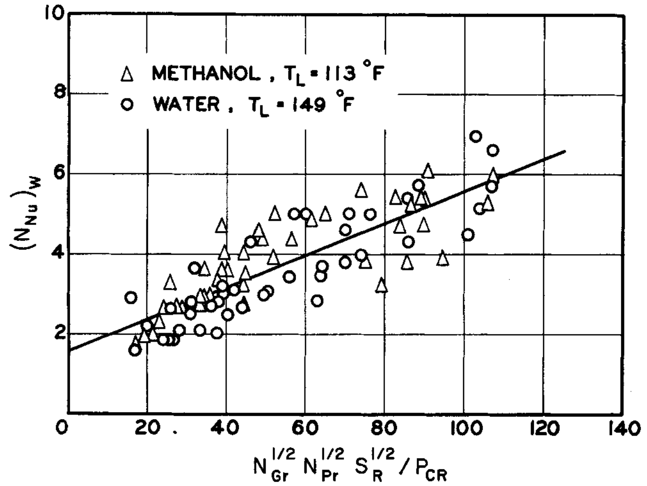

Fig. 12. Correlation of heat transfer data in the low heat flux region, f = 44.1 kcycles/sec.

isothermal conditions. The wire temperature effect was included in the Grashof number for heat transfer results in the low heat flux region. This would explain the high exponent for the Grashof number in Equation (2). At higher wire temperatures, the frequency of formation and the activity of cavitation bubbles were increased. The bubble content also changed from mainly gas to mainly vapor. The mechanism of heat transfer became similar to that in nucleate boiling without vibration. Equation (2) is no longer adequate to account for the wire temperature effect when the temperature is above that for incipient boiling. A Reynolds number similar to that in nucleate boiling (*12, 13*) for the cavitation bubbles was postulated. The cavitation bubble diameter approximated by Equation (1) was used as the characteristic length in the Reynolds number. The Reynolds number is then defined as

$$N_{Re} = \frac{D_B q \rho_L}{A \rho_v \lambda \mu_L} \tag{3}$$

Using a Nusselt number based on the cavitation bubble diameter, the heat transfer results at wire temperatures above that for incipient boiling were correlated. The correlation takes the form of

$$(N_{Nu})_B = C_3 \frac{{N_{Re}}^{1/2} {N_{Pr}}^{2/3} \; {S_R}^{1/2}}{P_{CR}} + C_4 \tag{4}$$

The liquid properties in dimensionless groups in both Equations (2) and (4) were evaluated at the arithmetic mean temperature of the wire and the bulk liquid. The correlation for 44.1 kcycles/sec. is shown in Figure 14. The slope and intercept of Equation (4) were obtained in the same manner as that of Equation (2). It was impossible to correlate heat transfer results from different frequencies with a single equation because the exact relationship between critical sound pressure and frequency of the ultrasonic field has not been found. In addition, the normalized plots of $(N_{Nu})_w/(N_{Nu})_o$ where $(N_{Nu})_o$ is the Nusselt number for the wire when there was no vibration were also prepared for the low heat flux data and one such plot is shown in Figure 15. No normalized plot was prepared for the high heat flux data because an accurate determination of heat transfer coefficients in nucleate boiling region without vibration was extremely difficult. While the normalized plots in the low heat flux region showed an increase in heat transfer coefficient as the wire temperature increased, the reverse would be expected in the high heat flux region.

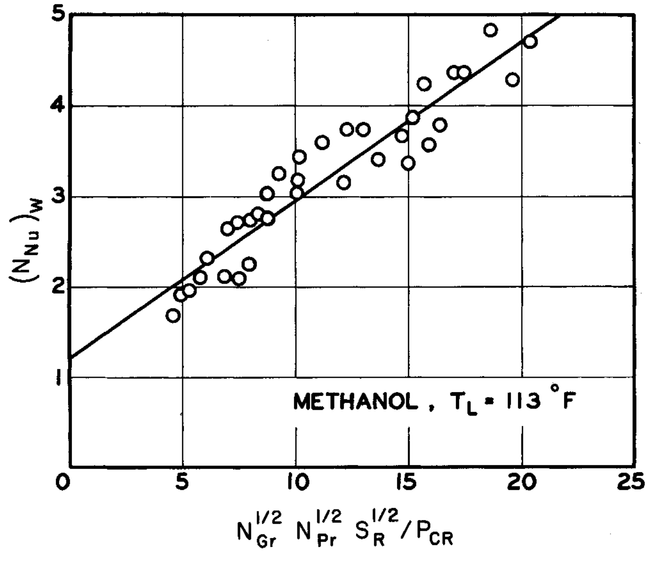

Fig. 13. Correlation of heat transfer data in the low heat flux region, f = 306 kcycles/sec.

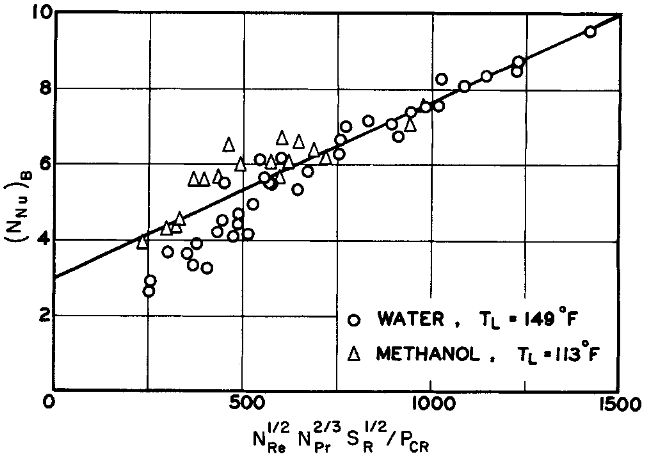

Fig. 14. Correlation of heat transfer data in the high heat flux region, f = 44.1 kcycles/sec.

It should be emphasized that the choice of the wire temperature at incipient boiling to separate the heat transfer data into two groups was purely an arbitrary one. A convenient basis would be the cavitation bubble content consisting of 50% gas and 50% vapor. This criterion was not used because it was difficult to measure the actual bubble content.

The heat transfer coefficients in both Equations (2) and (4) were found to be directly proportional to the

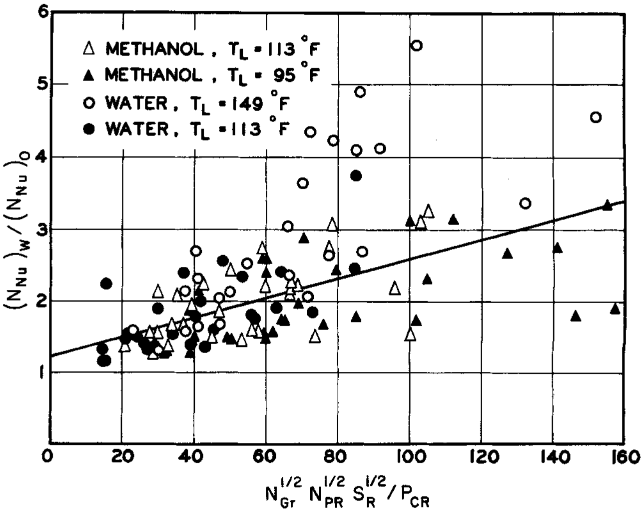

Fig. 15. Correlation of heat transfer data in the low heat flux region in terms of a normalized Nusselt number, f = 20.6 kcycles/sec.

square root of the percentage of soil removed. In the penetration theory proposed by Danckwerts (*14, 15*), it is shown that the mass transfer coefficient is inversely proportional to the square root of the time of contact between the liquid and the gas phase. The penetration theory assumes that the interface is continuously replaced by eddies so that fresh surface will be formed continuously at a constant rate. The reciprocal of the contact time is then shown to be the fractional rate of surface renewal. Consequently, the mass transfer coefficient is proportional to the square root of the fractional rate of surface renewal, which depends on the degree of turbulence in the liquid. From the analogy of heat and mass transfer, it appears that the percentage of soil removed is directly related to the intensity of turbulence resulting from cavitation in a liquid under ultrasonic vibrations. The mechanism of cavitation damage has been shown to be the result of the collapse of cavitation bubbles near and on a solid surface (*16*). The percentage of soil removed can then be interpreted as a measure of the rate of formation (collapse) of cavitation bubbles which becomes a measure of the turbulent intensity in the liquid.

Bebchuk, et al. (*17*) have shown that cavitation damage increased directly with the square of the sound pressure amplitude. This renders the term $(S_R)^{1/2}/P_{CR}$ dimensionless as the percentage of soil removed becomes directly proportional to the square of the sound pressure amplitude. The dimensionless term $S_R{}^{1/2}/P_{CR}$ gives a measure of the cavitation bubble activity for different liquids at different temperatures.

CONCLUSIONS

1. There existed a critical sound pressure, depending on the liquid used and its temperature, the frequency of the ultrasonic field and the heat transfer surface temperature, below which the effects of ultrasonic vibrations on heat transfer were negligible.
2. Above the critical sound pressure, the effects of ultrasonic vibrations on heat transfer to liquids varied from an 800% increase in heat transfer coefficient in the natural convection region to a negligible increase in the well-developed nucleate boiling.
3. The increase in heat transfer coefficient was due to the intense turbulence resulting from the radial oscillations as well as the rapid and erratic motion of the cavitation bubbles on the heat transfer surface. Under the present experimental conditions, it was impossbile to determine the frequency of generation of the cavitation bubbles and the number of active sites (if there was any) on the heat transfer surface.
4. The increase in heat transfer coefficient depended on the liquid used as well as its temperature. Liquid with low gas solubility would yield higher heat transfer coefficients and higher heat transfer rates would be obtained in liquid at a higher temperature.
5. The effect of frequency of the ultrasonic field was negligible if the same cavitation activity in the liquid was used. In order to achieve the same cavitation activity, more ultrasonic energy was required when the frequency was increased.

ACKNOWLEDGMENT

The authors are indebted to Dr. M. E. Weber for useful discussions and advice. Financial assistance received by S. W. Wong from the National Research Council of Canada is gratefully acknowledged.

NOTATION

A = surface area, ft.
c_p = specific heat, B.t.u./lb. °F.
C_1, C_2, C_3, C_4 = constants
D_w = wire diameter, ft.
D_B = cavitation bubble diameter, ft.
f = frequency of ultrasonic field, kcycles/sec.
g = acceleration due to gravity, ft./hr.^{2}
h = heat transfer coefficient, B.t.u./hr. sq.ft. °F.
k = thermal conductivity, B.t.u./ft. hr. °F.
P_{CR} = critical sound pressure, atm.
P_o = ambient pressure, atm.
P_s = rms sound pressure, atm.
q = heat transfer rate, B.t.u./hr.
R = resonance radius, ft.
S_R = percentage of soil removed, %
T_W = wire temperature, °F.
W_A = apparent electrical power, w.

Dimensionless Groups

N_{Gr} Grashof number, $g\beta \; \rho_L{}^2 D_W{}^3 \Delta T/\mu^2$
$(N_{Nu})_B$ Nusselt number, hD_B/k
$(N_{Nu})_o$ Nusselt number without vibration
$(N_{Nu})_W$ Nusselt number, hD_w/k
N_{Pr} Prandtl number, $\mu c_p/k$
N_{Re} Reynolds number, $D_B q \; \rho_L/A\rho_v\lambda\mu_L$

Greek Letters

β = coefficient of thermal expansion of fluid, °F.$^{-1}$
ΔT = temperature difference ($\Delta T = T_W - T_L$), °F.
γ = specific heat ratio
λ = latent heat of vaporization, B.t.u./lb.
μ = viscosity, lb./ft. hr.
ρ = density, lb./cu.ft.

Subscripts

B = cavitation bubble
L = liquid
v = vapor
w = wire

LITERATURE CITED

1. Larson, M. B., and A. L. London, *Am. Soc. Mech. Eng:, paper 62-HT-44* (1962).
2. Robinson, G. C., C. M. McClure, and R. Hendricks, *Bull. Am. Ceramic Soc.*, **37**, 399 (1958).
3. Isakoff, S. E., "Proc. Heat Transfer Fluid Mech. Inst.," p. 15, Stanford Univ. Press, Calif. (1956).
4. Romie, F. E., and C. A. Aronson, *Adv. Tech. Lab. Rept. ATL-A-123* (July, 1961).
5. Ornatskii, A. P., and V. K. Shcherbakov, *Teploenerg.*, **6**, 84 (1959).
6. Chon, W. Y., and S. W. Wong, paper presented at the *European Conv. Chem.* Eng., and the *Achema-Congress*, Frankfurt, Germany (June, 1967).
7. Wong, S. W., Ph.D. thesis, McGill Univ., Montreal, Canada, (1967).
8. Esche, R., *Akust, Beihefte*, **4**, 208 (1952).
9. Barger, J. E., *Acoustic Res. Lab., Tech. Memo no. 57*, Harvard Univ., Cambridge, Mass. (April, 1964).
10. Minnaert, M., *Phil. Mag.*, **16**, 235 (1933).
11. McAdams, W. H., "*Heat Transmission*," p. 176, McGraw-Hill, New York (1954).
12. Jakob, M., *Mech. Eng.*, **58**, 643, 729 (1936).
13. Rohsenow, W., *Trans. Am. Soc. Mech. Engrs.*, **74**, 969 (1952).
14. Danckwerts, P. V., *Ind. Eng. Chem.*, **43**, 1460 (1951).
15. ——— *AIChE J.*, **1**, 456 (1955).
16. Naude, C. F., and A. T. Ellis, *Trans. Am. Soc. Mech. Engrs.*, **D83**, 648 (1961).
17. Bebchuk, A. S., I. I. Borisov, and L. D. Rosenberg, *Soviet Phys. Acoust.*, **4**, 372 (1958).

Manuscript received August 2, 1967; revision received February 28, 1968; paper accepted February 29, 1968. Paper presented at AIChE New York City Meeting.